

Preprint of:

D. K. Gramotnev, M. L. Mather and T. A. Nieminen

“Anomalous absorption of bulk shear sagittal acoustic waves in a layered structure with viscous fluid”

Ultrasonics **41**, 197–205 (2003)

Anomalous absorption of bulk shear sagittal acoustic waves in a layered structure with viscous fluid

Dmitri K. Gramotnev, Melissa L. Mather and Timo A. Nieminen

Applied Optics Program, School of Physical and Chemical Sciences, Queensland University of Technology, GPO Box 2434, Brisbane, QLD 4001, Australia; e-mail: d.gramotnev@qut.edu.au

Abstract

It is demonstrated theoretically that the absorptivity of bulk shear sagittal waves by an ultra-thin layer of viscous fluid between two different elastic media has a strong maximum (in some cases as good as 100%) at an optimal layer thickness. This thickness is usually much smaller than the penetration depths and lengths of transverse and longitudinal waves in the fluid. The angular dependencies of the absorptivity are demonstrated to have significant and unusual structure near critical angles of incidence. The effect of non-Newtonian properties and non-uniformities of the fluid layer on the absorptivity is also investigated. In particular, it is shown that the absorption in a thin layer of viscous fluid is much more sensitive to non-zero relaxation time(s) in the fluid layer than the absorption at an isolated solid-fluid interface.

1 Introduction

One of the most important areas of application of acoustic waves is related to non-destructive evaluation and development of highly sensitive ultrasonic measurement techniques and sensors. This is the main reason for the intensive theoretical and experimental research in the area of propagation and interaction of various types of ultrasound waves near different kinds of interfaces, layered structures, defects, structural imperfections, etc. This includes theoretical and experimental investigations of interaction of acoustic waves with imperfect interfaces and sets of cracks or inclusions [1-5], slipping contacts [3,4], sliding contacts [6,7], bonding layers between two elastic media [8,9], propagation and interaction of acoustic waves near solid-fluid interfaces [10-17], etc. In these cases, various approaches based on spring boundary conditions [1,2,4,5], transfer matrix approach [8,9,19], equivalent boundary conditions [8,9,20], Stroh formalism [6,7], etc. have been developed and used.

One of the most important areas of application of acoustic waves is related to the development of new highly sensitive viscosity sensors and techniques for diagnostics of fluids and solid-fluid interfaces and fluid layers [4,10-18]. Major advantages of using acoustic waves for these applications are related to a possibility of diagnostics of small amounts of fluids, investigation of fluids in the immediate proximity of solid interfaces (i.e., analysis of processes of interaction between a fluid and a solid), possibility of sensor miniaturization and increased sensitivity.

In terms of development of new viscosity sensors and fluid diagnostics techniques, sensitivity of measurements is of prime importance. Surface acoustic waves usually provide higher sensitivity than bulk waves, because surface waves can easily be kept in contact with a fluid for a long time as they propagate along a solid-fluid interface. Therefore, ultrasonic viscosity sensors and diagnostic techniques are usually based on surface acoustic waves [12-14]. However, in some applications it may be more convenient to use bulk acoustic waves. Their main advantages over surface acoustic

waves are related to the absence of additional structures (such as generating and receiving interdigital transducers or periodic structures) at the solid-fluid interface, and much higher spatial resolution of measurements. Therefore, if we are able to improve sensitivity of viscosity sensors using bulk acoustic waves, these devices will be much more competitive as compared to surface acoustic wave sensors. This can be achieved using the anomalous absorption (AA) of acoustic waves by a thin layer of viscous fluid enclosed between two solid media [21-28]. Moreover, application of AA for viscosity sensor design may have additional advantages related to a possibility of diagnostics of extremely small (less than $\approx 10^{-5} \text{ cm}^3$) amounts of fluids, precise high frequency and low frequency analysis of solid-fluid interfaces and areas of fluid in the immediate proximity to the interface, and acoustic diagnostics of frictional contacts and lubricants. In addition, AA may be useful for the development of new techniques for non-destructive evaluation.

AA is characterized by a very strong increase in the absorptivity of the incident wave by the fluid layer with decreasing thickness of the layer (this is the reason for a substantial increase in the sensitivity of viscosity sensors using AA). The absorptivity reaches a maximum at an optimal layer thickness, and then quickly goes to zero as the layer thickness tends to zero [21-28]. The optimal layer thickness is usually much smaller than penetration depths and lengths of transverse and longitudinal waves in the fluid [21-28]. Therefore, AA cannot be explained by the attenuated total reflection or resonant interference of bulk waves in the layered structure. It was explained by a significant increase of the fluid velocity gradient in the layer when the thickness of the layer is decreased [21-28]. As a result, the dissipation in a unit volume of the fluid, which is proportional to the square of the velocity gradient, must also increase substantially. On the other hand, decreasing layer thickness results in decreasing volume in which the dissipation takes place. Thus the overall dissipation must have a tendency to decrease with decreasing layer thickness. The competition of these two opposing mechanisms results in an optimal layer thickness at which the absorptivity is maximal [21-28].

The theoretical analysis of AA has been carried out for both longitudinal [24,27] and shear [21-23,25,26] bulk acoustic waves. Coefficients of absorption, reflection, transmission and transformation have been analysed as functions of angle of incidence, fluid layer thickness, frequency and parameters of the media in contact. Unusually strong absorption at the optimal layer thickness has been predicted for all types of acoustic waves [21-28]. The frictional contact approximation, which in many cases allows accurate analytical solution of the problem, has been introduced and justified [21-26]. This approximation is equivalent to the spring boundary conditions [1-5], but with the zero inertial load at the contact and imaginary (for Newtonian fluid) or complex (for non-Newtonian fluid) spring constants for tangential displacements. Optimisation of structural parameters for maximal absorptivity in the layer has been carried out. The effects of non-Newtonian properties of the fluid on AA has been investigated for longitudinal waves [27] and bulk shear waves polarized normally to the plane of incidence [26]. More recently, experimental investigation of AA, and verification of the theoretical predictions for bulk shear waves at normal incidence have been carried out [28].

However, although the analysis of AA of bulk acoustic waves has been quite thorough, there has been little attention paid to AA of shear sagittal acoustic waves (i.e., shear waves polarized in the plane of incidence). To our knowledge, only one paper has made an attempt of the theoretical analysis of AA of shear sagittal waves [23]. In addition, this paper was only confined to two special cases when a Newtonian fluid layer is placed either between two identical elastic media, or between two media, one of which can be regarded as infinitely rigid [23]. At the same time, in practice, we often come across situations where a thin fluid layer is enclosed between two similar but different elastic materials (e.g., in the case of a frictional contact between different objects). Moreover, it can be expected that AA of shear sagittal waves in the vicinity of critical angles of incidence will result in interesting effects that are similar to those for longitudinal waves and shear waves polarized perpendicular to the plane of incidence [21,24, 26,27]. In addition, AA of shear sagittal acoustic waves is anticipated to be affected by non-Newtonian properties of fluids at high frequencies. Neither of these questions has been investigated theoretically to date.

Therefore, the aim of this paper is to investigate theoretically AA of bulk shear sagittal acoustic waves by a layer of Newtonian or non-Newtonian fluid between two different elastic media. The optimal layer thickness and the coefficients of reflection, transmission, transformation and absorption will

be analysed numerically as functions of incidence angle, frequency and parameters of the media in contact. Significant and unusual structure of the dependencies of absorptivity on the angle of incidence near three critical angles is predicted. Comparison with the case of identical elastic media [23] is carried out.

2 Basic equations and conditions

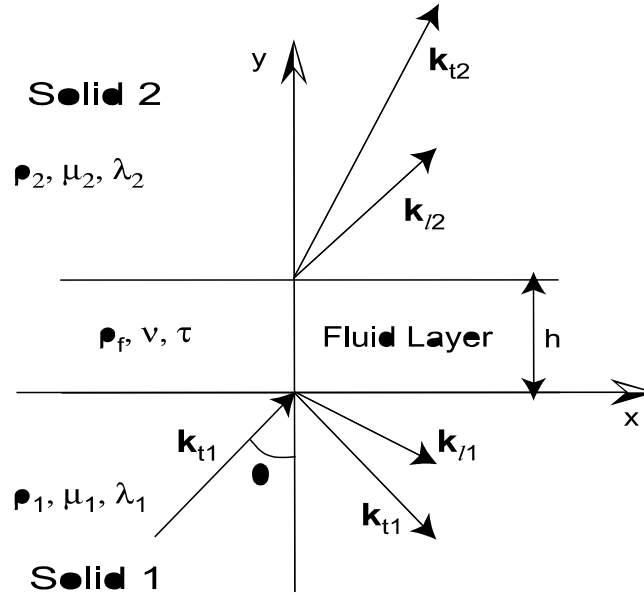


Figure 1: The structure with the anomalous absorption of bulk sagittal shear waves in a fluid layer between two elastic media.

The analysed structure with a fluid layer enclosed between two elastic halfspaces, is presented in Fig. 1. A bulk shear sagittal wave propagating in the first elastic medium is incident onto the fluid layer at an angle θ . As a result, in the first halfspace there are two reflected waves, one of which is a shear sagittal wave and the other is a longitudinal wave. Similarly, in the second elastic medium there are two transmitted waves, one of which is a shear sagittal wave and the other is a longitudinal wave (Fig. 1). The elastic media 1 and 2 are characterized by the Lamé coefficients $\lambda_{1,2}$, $\mu_{1,2}$ and densities $\rho_{1,2}$, respectively. The vectors $\mathbf{k}_{l1,2}$ are the wave vectors of the longitudinal waves ($k_{l1,2} = \omega[\rho_{1,2}/(\lambda_{1,2} + 2\mu_{1,2})]^{1/2}$), and $\mathbf{k}_{t1,2}$ are the wave vectors of the shear waves ($k_{t1,2} = \omega[\rho_{1,2}/\mu_{1,2}]^{1/2}$) in elastic media 1 and 2, respectively, ω is the angular frequency. The fluid layer has the thickness h , kinematic viscosity ν and density ρ_f . The system of coordinates is presented in Fig. 1.

All viscous fluids are characterized by one or more times of relaxation, τ_m ($m = 1, 2, \dots$), of shear stresses [10,11]. If the frequency $\omega \ll \tau_m^{-1}$ for all values of m , then the relaxation times can be neglected and the fluid is Newtonian. If $\omega \approx \tau_m^{-1}$ at least for one m , then the fluid is characterized not only by a shear viscosity, but also by some non-zero shear modulus [10,11,26]. Such fluids are called non-Newtonian fluids.

The rigorous analysis of the interaction of an incident shear sagittal wave with a viscoelastic layer of non-Newtonian fluid of arbitrary thickness can be carried out using the transfer matrix approach [8,9,19]. However, as we will see below, the absorptivity in the fluid layer is usually strong if the layer thickness, h , is small compared to the penetration depth and length of the shear acoustic wave in the fluid. If, in addition, the effect of the mass of the fluid layer on the wave propagation is negligible, then the transfer matrix approach results in the following approximate boundary conditions for the layer [5,8]:

$$\sigma_{1yy} = K_n(U_{1y} - U_{2y}), \sigma_{1xy} = K_t(U_{1x} - U_{2x}), \sigma_{1yy} = \sigma_{2yy}, \sigma_{1xy} = \sigma_{2xy}, \quad (1)$$

where $\sigma_{1,2ik}$ are the strain tensor components, and $U_{1,2}$ are the displacement vectors in elastic halfspaces 1 and 2, respectively, $K_t = i\omega b/h$, $K_n = C/h$ (these coefficients also represent spring constants

in the spring boundary conditions [1-5]), ω is the frequency of the incident wave, C is the bulk modulus of the fluid ($C = v^2 \rho_f$, v is the speed of longitudinal acoustic waves in the fluid), and

$$b = \sum_m \frac{\mu_{\infty m} \tau_m}{i\omega \tau_m - 1} \quad (2)$$

where the summation is taken over all different relaxation processes in the fluid, $\mu_{\infty m}$ are the contributions to the overall shear modulus, $\mu_{\infty} = \sum_m \mu_{\infty m}$, of the fluid at $\omega \rightarrow +\infty$ from each of the relaxation processes.

Usually, the speed of longitudinal waves in a viscous fluid is much larger than the speed of shear waves caused by shear viscosity, which means that

$$|C/(b\omega)| \gg 1. \quad (3)$$

or $|K_n/K_t| \gg 1$. Therefore, equations (1) give $U_{1y} - U_{2y} \ll U_{1x} - U_{2x}$. and the displacements that are normal to the layer must be approximately the same at the layer boundaries $y = 0$ and $y = h$ (Fig. 1). Thus the first of the boundary conditions (1) can be reduced as $U_{1y} = U_{2y}$. Introducing also tangential velocities of the layer boundaries $\partial U_{1,2x}/\partial t = -i\omega U_{1,2x}$, gives

$$\sigma_{1yy} = \sigma_{2yy}, U_{1y} = U_{2y}, \sigma_{1xy} = \sigma_{2xy}, \sigma_{1xy} = W(\partial U_{2x}/\partial t - \partial U_{1x}/\partial t)_{y=0} \quad (4)$$

where

$$W = -b/h. \quad (5)$$

Boundary conditions (4) mean that the fluid layer has been replaced by an immediate contact of two solid halfspaces with friction, the coefficient of which is given by Eq. (5). Indeed, normal displacements and tangential and normal stresses are continuous across the contact (layer), and the tangential stresses are proportional to the relative velocity of the surfaces in contact. The coefficient of proportionality, W , is the coefficient of friction, which is real for Newtonian fluid layers and complex for non-Newtonian fluids (see Eq. (5)). Note that this procedure is similar to that used for the approximation of a bonding layer between two elastic media by some special boundary conditions (e.g., spring boundary conditions), depending on the properties of the layer [1-5,8,9,20].

As has been mentioned above, the main applicability condition for the frictional contact approximation (represented by conditions (4)) to a fluid layer between two elastic media is that the layer thickness h must be noticeably smaller than the magnitude of the complex penetration depth a of the shear wave into the fluid:

$$h|\alpha| \ll 1, \quad (6)$$

where

$$\alpha^2 = -i\omega\rho_f/b + k_{11}^2 \sin^2 \theta. \quad (7)$$

However, conditions (3) and (6) are necessary but not sufficient for the validity of boundary conditions (1) and (4). It is also necessary to assume that the mass of the layer can be neglected [8,9]. This can be done if, in addition to conditions (3) and (6), the shear impedance of the fluid is much smaller than the shear impedances of the surrounding elastic media:

$$|b\alpha| \ll (\rho_1\mu_1)^{1/2}, (\rho_2\mu_2)^{1/2} \quad (8)$$

(compare with the similar conditions for the frictional contact approximation for shear acoustic waves polarized perpendicular to the plane of incidence in a thin layer of Newtonian and non-Newtonian fluids [21,26]).

Note that at lower frequencies ($\ll 100$ MHz) conditions (3) and (8) can be breached only if the viscosity, density, and/or relaxation times of the fluid are unusually large, or the shear modulus of at least one of the surrounding elastic media is unusually small (rubber-like material). For commonly used fluids and solids at not very high frequencies, conditions (3) and (8) can easily be satisfied and the main condition for the frictional contact approximation is given by inequality (6).

Substituting the solutions to the wave equations in elastic media in the form of one incident, two reflected and two transmitted waves (see Fig. 1) into boundary conditions (4), we obtain a set of four linear algebraic equations with four unknown wave amplitudes. The energy coefficients of reflection, transmission and transformation were determined as the ratios of the y -components of the Poynting vectors in the relevant reflected or transmitted waves to the y -component of the Poynting vector in the incident wave. In this case the wave absorptivity in the layer is given by:

$$M = 1 - T - R - K_1 - K_2, \quad (9)$$

where T is the transmissivity, R is the reflectivity, K_1 is the coefficient of transformation of the incident transverse wave into a reflected longitudinal wave in the first elastic medium, and K_2 is the coefficient of transformation in the second elastic medium.

One of the significant advantages of the presented frictional contact approximation is that it allows simple analysis of AA in non-uniform thin fluid layers. If fluid parameters such as viscosity, density, relaxation time(s) vary across the layer, for example due to interaction of the fluid with the solid surfaces, then the parameter b determined by Eq. (2) is a function of the y -coordinate (Fig. 1). As shown in paper [26], the frictional coefficient for such a non-uniform layer of non-Newtonian fluid of thickness h is given by the equation:

$$W = - \left(\int_0^h b^{-1} dy \right)^{-1}. \quad (10)$$

In this case condition (6) has to be written as [26]:

$$\int_0^h |\alpha| dx \ll 1 \quad (11)$$

and in conditions (3) and (8) b must be replaced by $\max(|b|)$.

In the frictional contact approximation, the coefficient of friction is the only parameter that represents properties of the fluid layer. Therefore, if we use Eq. (10) for the frictional coefficient, then all other equations determining AA in a non-uniform layer will remain the same as for uniform layers.

3 Numerical analysis

An attempt to carry out analytical analysis of AA of shear sagittal waves was made in paper [23] for the special case of a uniform Newtonian fluid layer between two identical elastic media. However, analytical analysis becomes much more involved if more complicated structures are considered and, therefore, numerical analysis of AA has been used in this paper. In addition, since in the frictional contact approximation non-uniform fluid layers can be analysed in the same way as uniform layers (with the use of Eq. (10)), only examples with uniform fluid layers will be considered in this section.

As an example, consider a structure with a thin uniform layer of poly-1-butene-16 (with 16 repeat units and average molecular weight 640 [10]), enclosed between two solid halfspaces. The parameters of the fluid layer are $\rho_f \approx 0.88 \text{ g/cm}^3$, $\nu \approx 57 \text{ cm}^2/\text{s}$, and $\tau \approx 6.33 \times 10^{-9} \text{ s}$ [10] (only one relaxation time is taken into account, $\mu_\infty = \rho_f \nu / \tau$).

If the first elastic medium is made of silica ($\rho_1 = 2.2 \text{ g/cm}^3$, $\mu_1 = 3.11 \times 10^{11} \text{ dyne/cm}^2$), and the second elastic medium is made of tin ($\rho_2 = 7.3 \text{ g/cm}^3$, $\mu_2 = 2.11 \times 10^{11} \text{ dyne/cm}^2$), then the structure will be called silica–poly-1-butene-16–tin. Similarly, if the first medium is tin and the second is silica, then we will have a tin–poly-1-butene-16–silica structure, etc.

Fig. 2 presents typical dependencies of the absorptivity M on layer thickness h for two different structures: tin–fluid–silica (curves 1-4) and silica–fluid–tin (curves 5 and 6). The angles of incidence are $\theta = \theta_{cl}(\text{tin}) \approx 38.504^\circ$ (curves 1 and 2), $\theta = 70^\circ$ (curves 3, 4, and 6), and $\theta = \theta_{cl}(\text{silica}) \approx 39.046^\circ$ (curve 5), where θ_{cl} is the critical angle at which the reflected longitudinal wave in medium 1 propagates parallel to the layer. Curves 2 and 4 are presented for the non-Newtonian fluid layer made

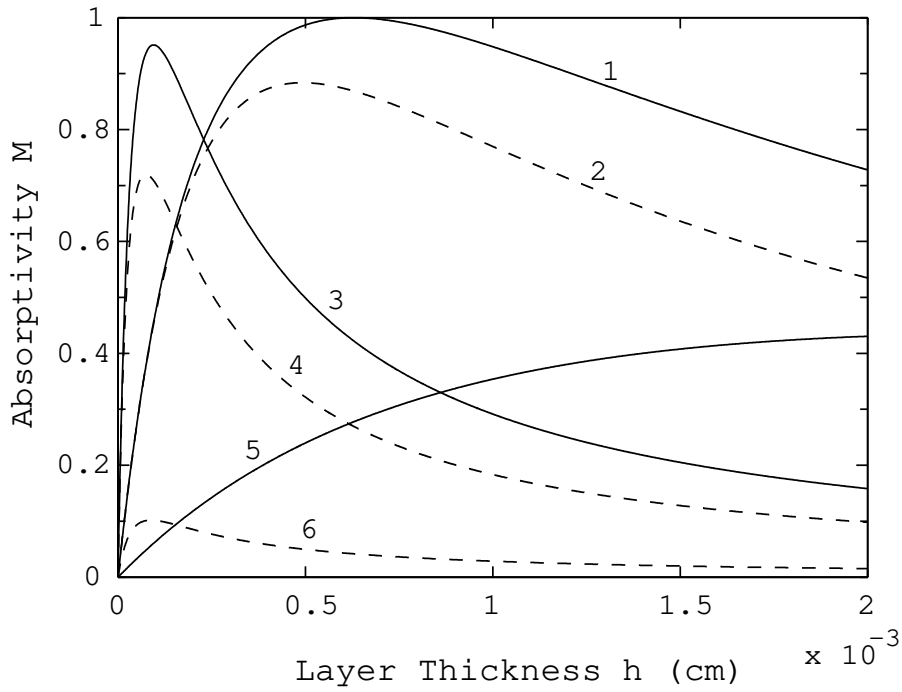


Figure 2: The dependencies of the absorptivity on layer thickness for two different structures: tin-fluid-silica (curves 1-4), and silica-fluid-tin (curves 5 and 6). The fluid layer: poly-1-butene-16 with $\rho_f = 0.88 \text{ g/cm}^3$, $\nu = 57 \text{ cm}^2/\text{s}$, $\tau = 6.33 \times 10^{-9} \text{ s}$ [10] and $\omega/2\pi = 20 \text{ MHz}$ (curves 2 and 4); the Newtonian fluid with the same ρ_f and ν but $\omega\tau \ll 1$ (curves 1, 3, 5, and 6). Angles of incidence $\theta = \theta_{cl}(\text{tin}) \approx 38.504^\circ$ (curves 1 and 2), $\theta = 70^\circ$ (curves 3, 4, and 6), $\theta = \theta_{cl}(\text{silica}) \approx 39.046^\circ$ (curve 5).

of poly-1-butene-16 with $\tau = 6.33 \times 10^{-9} \text{ s}$ at the acoustic frequency $\omega/2\pi = 20 \text{ MHz}$ ($\omega\tau \approx 0.8$), while curves 1, 3, 5, and 6 are presented for the Newtonian fluid layer with the same ρ_f and ν as poly-1-butene-16, but at $\omega\tau \ll 1$. Note that in the frictional contact approximation all curves for Newtonian fluid layers (e.g., curves 1, 3, 5, and 6 in Fig. 2) are frequency independent—see also [21,23,24,26,27].

All the curves in Fig. 2 display the behaviour typical of AA (see also [21-27]). The absorptivity strongly increases with decreasing layer thickness, reaches a relatively broad maximum at an optimal thickness, h_m , and then quickly goes to zero as the layer thickness tends to zero (Fig. 2). Note that for curve 5 the absorptivity maximum is reached at the optimal thickness $h_m \approx 25 \mu\text{m}$ and therefore cannot be seen in Fig. 2. The maximums of the absorptivity dependencies are broad, which reflects the non-resonant character of AA (see also [21-26]). The absorptivity curves for a non-Newtonian fluid are lower than for the corresponding Newtonian fluid (compare curves 1, 3 and 2, 4 in Fig. 2). This is the result of the general tendency: the larger the product $\omega\tau$, the smaller the absorptivity maximum due to AA. Note however that the difference between the curves for the Newtonian and non-Newtonian fluids is maximal at layer thicknesses near (or a few times larger than) the optimal thickness. If $h \ll h_m$ or $h \gg h_m$, the sensitivity of the absorptivity to non-zero relaxation time becomes noticeably weaker. That is why AA may especially be useful for the analysis of non-Newtonian properties of fluids (see also [28]).

Comparison of curves 1-4 and 5, 6 in Fig. 2 suggests that it is preferable to use structures with the first elastic medium having smaller speeds of acoustic waves than in the second medium. In this case stronger AA can be achieved (Fig. 2).

The angular dependencies of the optimal layer thickness, $h_m(\theta)$, for the silica-poly-1-butene-16-tin structure are presented in Fig. 3a. Curve 1 in Fig. 3a is for the poly-1-butene-16 layer with the assumption that $\omega\tau \ll 1$, while curves 2 and 3 are for the cases with $\tau = 6.33 \times 10^{-9} \text{ s}$ and the frequencies $\omega/2\pi = 20$ and 40 MHz , respectively. All three curves are characterized by strong maximums at the critical angle $\theta_{cl} \approx 39.046^\circ$. The values of these maximums are 25, 20, and $14 \mu\text{m}$ for

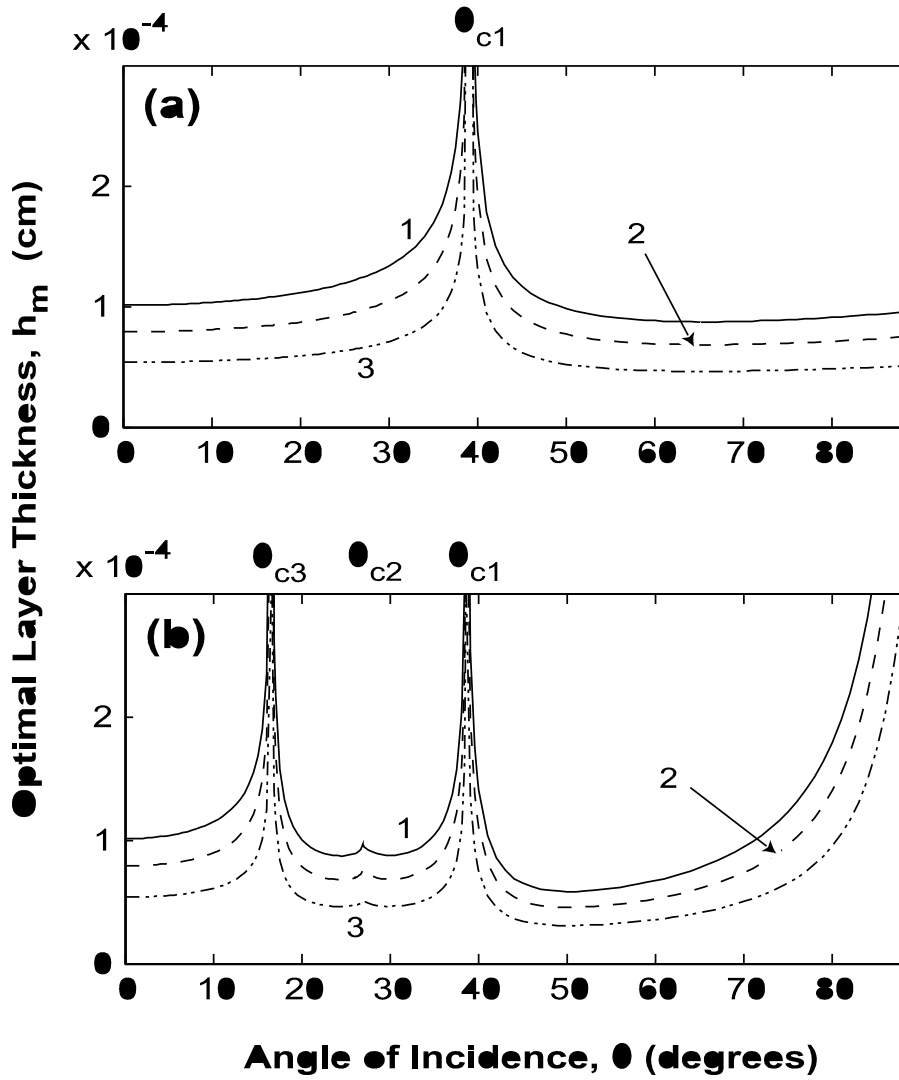


Figure 3: The angular dependencies of the optimal layer thickness for the silica-fluid-tin structure (a), and tin-fluid-silica structure (b). The fluid layer: (1) poly-1-butene-16 with $\tau = 1$ (Newtonian fluid); (2) poly-1-butene-16 with $\tau = 6.33 \times 10^{-9}$ s and $\omega/2\pi = 20$ MHz; (3) same as (2) but with $\omega/2\pi = 40$ MHz.

curves 1, 2, and 3, respectively. It can be seen that the effect of non-Newtonian properties of the fluid is the reduction in the optimal layer thickness (Fig. 3a).

Fig. 3b displays the dependencies $h_m(\theta)$ for the tin-poly-1-butene-16-silica structure for the frequencies $\omega/2\pi = 20$ MHz (curve 2) and $\omega/2\pi = 40$ MHz (curve 3). Curve 1 represents the same structure, but with $\omega\tau \ll 1$ (i.e., for the Newtonian fluid layer). The three maximums of each of these dependencies correspond to three critical angles of incidence in the considered structure. As has been mentioned, the first critical angle, $\theta_{c1} \approx 38.504^\circ$ corresponds to the reflected longitudinal wave in medium 1 (tin) propagating parallel to the layer ($\mathbf{k}_x = \mathbf{k}_{t1x} = \mathbf{k}_{l1}$). The second critical angle $\theta_{c2} \approx 26.9^\circ$ corresponds to the transmitted shear wave propagating parallel to the layer ($\mathbf{k}_x = \mathbf{k}_{t2}$). Finally, the third critical angle $\theta_{c3} \approx 16.55^\circ$ corresponds to the longitudinal wave in medium 2 propagating parallel to the layer (this happens when $\mathbf{k}_x = \mathbf{k}_{l2}$). If $\theta = \theta_{c1}$, then the optimal layer thickness for the Newtonian fluid (curve 1) is $6.9 \mu\text{m}$, while for curves 2 and 3 it is equal to 5.4 and $3.9 \mu\text{m}$, respectively. Similarly, if $\theta = \theta_{c3}$, then the optimal layer thickness for the Newtonian fluid reaches $25 \mu\text{m}$, while for curves 2 and 3 it is 20 and $14 \mu\text{m}$. At the second critical angle the optimal layer thicknesses are characterized by only a very minor peak (Fig. 3b).

The curves in Fig. 3b also demonstrate a reduction in the optimal layer thicknesses with increase of fluid relaxation time or frequency. This is similar to the tendency that has been observed in Fig. 3a.

Note again that curves 1 for Newtonian fluid layers in Fig. 3a and b are independent of frequency. The dependencies $h_m(\theta)$ in Fig. 3a are typical of structures where the speed of transverse waves in medium 1 is larger than the speed of longitudinal waves in medium 2 ($c_{t1} > c_{l2}$), whereas the dependencies in Fig. 3b are typical of structures where $c_{t1} < c_{l2}$.

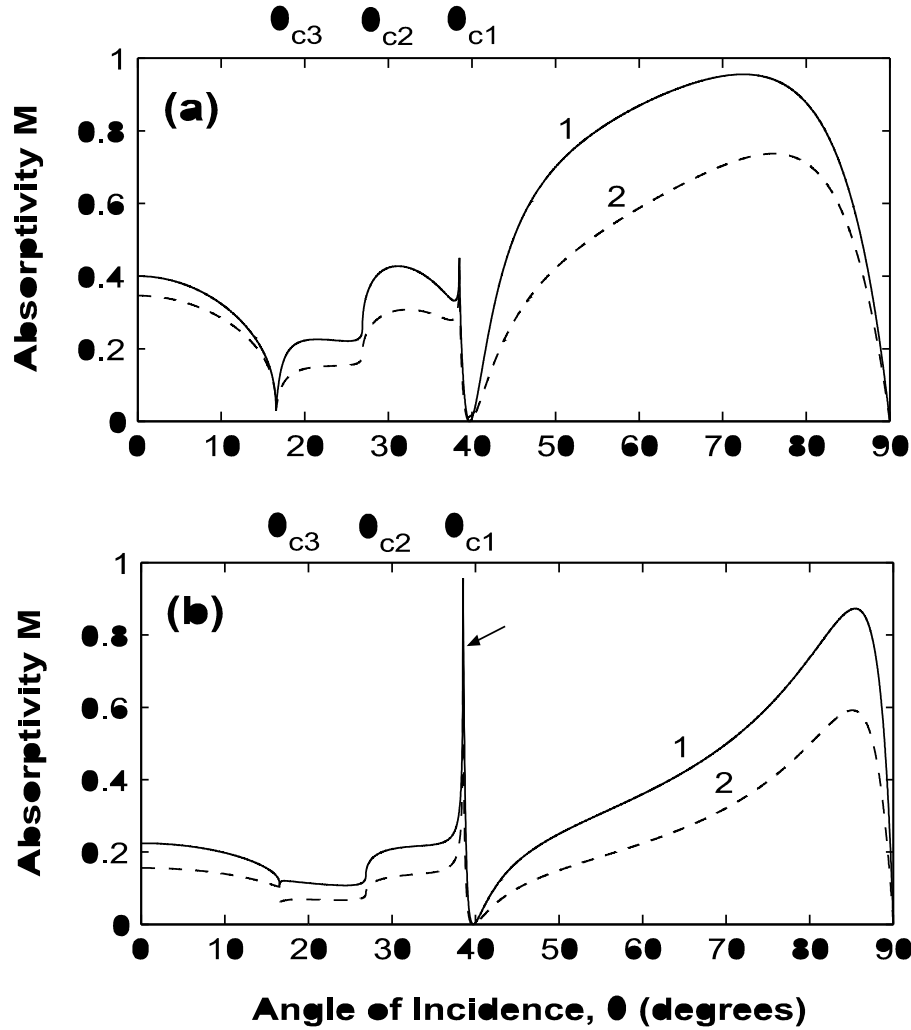


Figure 4: The angular dependencies of the absorptivity M for the tin–fluid–silica structure for the two layer thicknesses: (a) $h = 1\mu$, (b) $h = 5\mu$. The fluid layer: poly-1-butene-16 with $\omega\tau \ll 1$ (Newtonian fluid—curves 1); and poly-1-butene-16 with $\tau = 6.33 \times 10^{-9}$ s and $\omega/2\pi = 20$ MHz (curves 2). The arrow indicates the maximal value of the absorptivity for curve 2.

The dependencies of the absorptivity on angle of incidence for the tin–fluid–silica structure are presented in Fig. 4a and b for two different layer thicknesses: (a) $h = 1\mu$, and (b) $h = 5\mu$. Curves 1 are again for the Newtonian layer (i.e., poly-1-butene-16 with $\omega\tau \ll 1$), while curves 2 are for the non-Newtonian fluid layer with $\tau = 6.33 \times 10^{-9}$ s and $\omega/2\pi = 20$.

The most interesting feature of Fig. 4a and b is the sharp and strong maximum of absorptivity at the first critical angle (Fig. 4b) for both Newtonian and non-Newtonian fluids. It is important that this maximum is achieved at the same angle at which the optimal layer thickness also has a strong maximum (Fig. 3b). This behaviour is unique to AA of sagittal shear waves, since the usual tendency is that increasing optimal layer thickness (e.g., near the critical angle for shear waves polarized normally to the plane of incidence) results in a simultaneous decrease of the absorptivity maximum [21,22,26]. The coincidence of the maximums of the absorptivity and optimal layer thickness (Figs. 3b and 4b) may also be important for observation and application of AA in fluid layers with small viscosity, where optimal thickness may be unreasonably small [21,22,26].

Figs. 3b and 4a,b are typical for the case when the speed of longitudinal acoustic waves in medium

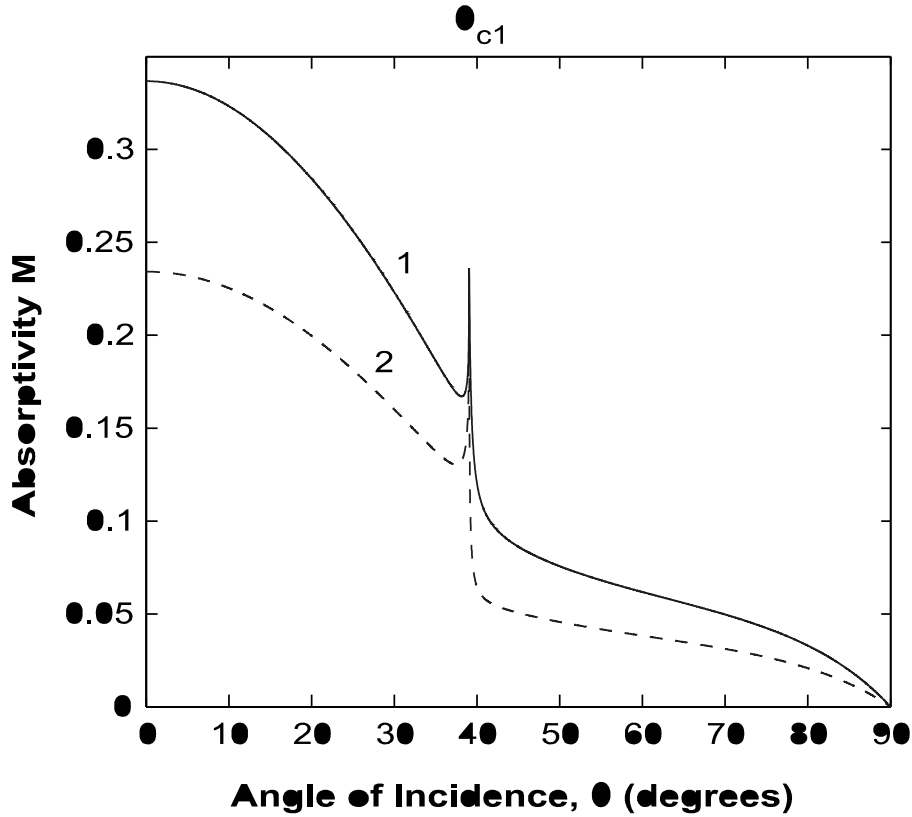


Figure 5: The angular dependencies of the absorptivity M for the tin–fluid–silica structure for the layer thickness $h = 5\mu\text{m}$. The fluid layer: (1) poly-1-butene-16 with $\omega\tau \ll 1$ (Newtonian fluid); (2) poly-1-butene-16 with $\tau = 6.33 \times 10^{-9}$ and $\omega/2\pi = 20\text{MHz}$.

1, c_{11} , is less than the speed of transverse waves in medium 2, c_{t2} , i.e., when three critical angles exist and $\theta_{c2,3} < \theta_{c1}$. If only one critical angle exists, i.e., if the speed of longitudinal waves in medium 2, c_{l2} , is smaller than the speed of the incident transverse wave, c_{t1} , (e.g., for the silica–fluid–tin structure), then the typical angular dependencies of the absorptivity are presented in Fig. 5 for the layer thickness $h = 5\mu\text{m}$ for Newtonian (curve 1) and non-Newtonian (curve 2) fluids. It can be seen that in this case the overall absorptivity is significantly smaller. However, a sharp (but smaller) maximum at the first (and the only) critical angle still exists for both Newtonian and non-Newtonian fluid layers (Fig. 5).

One may think that the sharp maximums of the angular dependencies of the absorptivity at the critical angles (Figs. 4 and 5) may have the same physical explanation as the maximums of conversion of a sagittal shear wave into a longitudinal wave at an interface between two media due to the generation of pseudo-surface-waves at the interface [20]. However, in our opinion, this interpretation is questionable. Indeed, the maximums of the longitudinal wave amplitudes in [20] occur at angles that are slightly (but noticeably) larger than the critical angle, whereas all the maximums in Figs. 3–5 and below occur precisely at the critical angles. Furthermore, it can be seen that the absorptivity due to AA at the angle corresponding to the maximal wave transformation [20] is substantially lower than its maximum value at the critical angle (Figs. 4 and 5). For example, for the sapphire–copper structure considered in [20] the maximum of the absorptivity due to AA (if there is a fluid layer between the elastic media) and the maximum of the wave transformation [20] hardly overlap. This suggests different physical nature of these maximums and effects.

At the same time, the sharp features of the angular dependencies of the reflected and refracted waves at the critical angles at a sliding contact between two elastic media [7] obviously have a relationship to the behaviour of the similar dependencies in the case of AA in a fluid layer at the same angles. However, it is necessary to stress out that AA does not exist on a sliding contact, because such a contact is non-dissipative (without friction) [7].

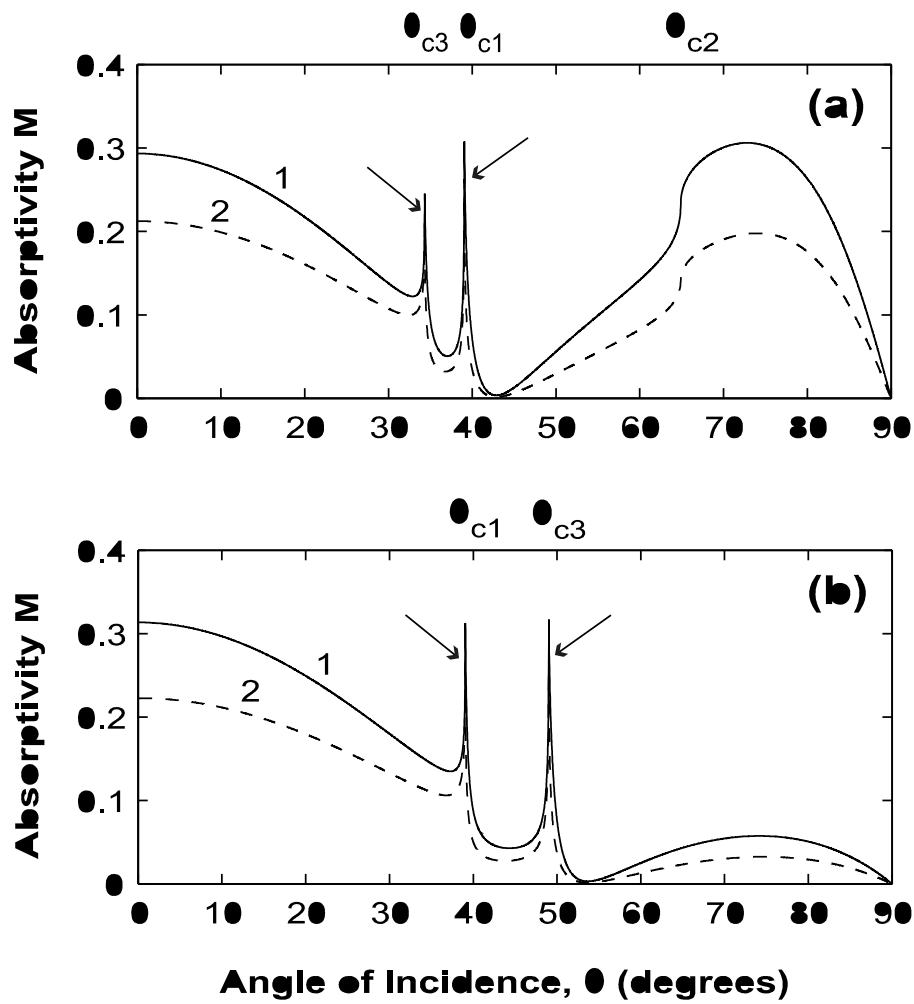


Figure 6: The angular dependencies of the absorptivity M in the structure silica–fluid–medium 2, where the parameters of the hypothetical medium 2 are: (a) $\rho_2 = 1.45 \text{ g/cm}^3$, $\mu_2 = 2.5 \times 10^{11} \text{ dyne/cm}^2$, $\lambda_2 = 1.45 \times 10^{11} \text{ dyne/cm}^2$; (b) $\rho_2 = 2.6 \text{ g/cm}^3$ and μ_2 and λ_2 are the same as in (a). The layer thickness is $h = 5 \mu\text{m}$. The fluid layer: poly-1-butene-16 with $\omega\tau \ll 1$ (Newtonian fluid—curves 1); and poly-1-butene-16 with $\tau = 6.33 \times 10^{-9}$ and $\omega/2\pi = 20 \text{ MHz}$ (curves 2). The arrows indicate the maximal values of the absorptivity for curves 2.

Fig. 6a and b present typical angular dependencies of the absorptivity for structures where $c_{t1} < c_{t2}$ and $c_{t2} < c_{t1} < c_{t2}$ (i.e., $\theta_{c3} < \theta_{c1} < \theta_{c2}$; $\theta_{c1} \approx 39.046^\circ$, $\theta_{c2} \approx 64.9^\circ$, $\theta_{c3} \approx 34.314^\circ$ —Fig. 6a), and $c_{t1} < c_{t2} < c_{t1}$ but $c_{t1} > c_{t2}$, i.e., $\theta_{c3} > \theta_{c1}$ and θ_{c2} does not exist ($\theta_{c1} \approx 39.046^\circ$, $\theta_{c3} \approx 49.015^\circ$ —Fig. 6b). It can be seen that in these cases the absorptivity is characterized by two sharp and strong maximums—at θ_{c1} (as in Figs. 4 and 5), and at θ_{c3} . Note however, that these maximums are not as strong as the maximum in Fig. 4b. In the tin–fluid–silica structure the absorptivity also experiences a sharp maximum at the angle $\theta = \theta_{c3}$, but at significantly larger layer thicknesses (e.g., at $h = 20 \mu\text{m}$) than those used for plotting Fig. 4a and b. This is the reason for not observing this maximum at $\theta = \theta_{c3} \approx 16.55^\circ$ in Fig. 4a and b. Thus, similar to the absorptivity maximum at $\theta = \theta_{c1}$, the maximum at $\theta = \theta_{c3}$ also coincides with a strong maximum in the optimal layer thickness (see Fig. 3b).

Note that the absorptivity maximum at the first critical angle has also been predicted for a Newtonian fluid layer between two identical elastic media [23]. However, in that case, the absorptivity maximum was restricted to 50% [23], whereas in the case of different media it can go as high as 100%—Figs. 2 and 4b. In addition, in the case of different elastic media we can obtain two sharp maximums at the first and the third critical angles—Fig. 6a and b. Actually, for identical elastic media these two maximums coincide with each other, giving only one maximum that can reach 50% [23]. Therefore,

an interesting question is what will happen to this maximum if the parameters of the two elastic media are only slightly different? How sensitive is AA to small variations of the elastic media? These questions are especially interesting due to the sharpness of the absorptivity maximum at $\theta = \theta_{c1}$, and due to small natural fluctuations of parameters of elastic media.

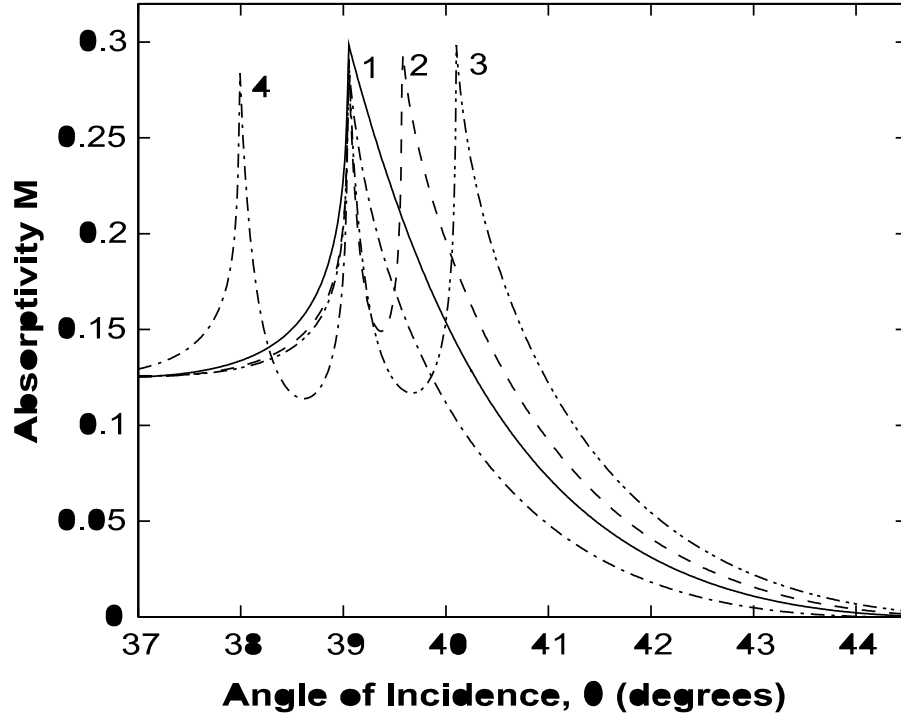


Figure 7: The angular dependencies of the absorptivity M in the structure silica–fluid–silica, where the density of the second silica halfspace ρ_2 is slightly different from the first halfspace: (1) $\rho_2 = \rho_1 = 2.2 \text{ g/cm}^3$, (2) $\rho_2 = 2.25 \text{ g/cm}^3$ and $\rho_1 = 2.2 \text{ g/cm}^3$, (3) $\rho_2 = 2.3 \text{ g/cm}^3$ and $\rho_1 = 2.2 \text{ g/cm}^3$, (4) $\rho_2 = 2.1 \text{ g/cm}^3$ and $\rho_1 = 2.2 \text{ g/cm}^3$. The layer thickness is $h = 5 \mu\text{m}$.

Therefore, Fig. 7 presents the angular dependencies of the absorptivity in a layer of poly-1-butene-16 (at $\omega\tau \ll 1$ of thickness $h = 5 \mu\text{m}$ between two silica halfspaces with small variations of the density of the second silica halfspace: (1) $\rho_2 = \rho_1 = 2.2 \text{ g/cm}^3$, (2) $\rho_2 = 2.25 \text{ g/cm}^3$ and $\rho_1 = 2.2 \text{ g/cm}^3$, (3) $\rho_2 = 2.3 \text{ g/cm}^3$ and $\rho_1 = 2.2 \text{ g/cm}^3$, (4) $\rho_2 = 2.1 \text{ g/cm}^3$ and $\rho_1 = 2.2 \text{ g/cm}^3$. The elastic modulae of both the silica halfspaces are assumed to be the same: $\mu_1 = \mu_2 = 3.11 \times 10^{11} \text{ dyne/cm}^2$, $\lambda_1 = \lambda_2 = 1.62 \times 10^{11} \text{ dyne/cm}^2$. It can be seen that in the case of different densities $\rho_1 \neq \rho_2$ (curves 2–4 in Fig. 7) the single maximum (curve 1) splits into two similar sharp maximums. The angular distance between these maximums increases with increasing difference between the densities of the elastic halfspaces, and the dip between the maximums becomes more pronounced (Fig. 7).

Finally, Fig. 8a and b present the frequency dependencies of the absorptivity maximum for the tin–poly-1-butene-16–silica (curves 1 and 2) and silica–poly-1-butene-16–tin (curves 3 and 4) structures for two different layer thicknesses $h = 1 \mu\text{m}$ (Fig. 8a) and $h = 5 \mu\text{m}$ (Fig. 8b) in the approximation of the frictional contact approximation. The short dashed lines parallel to the horizontal axis correspond to the Newtonian fluid layers with the same thicknesses, viscosity and density.

The main aspect that can be seen from Fig. 8a and b is that the non-Newtonian properties of the fluid produce significantly stronger effect on AA of sagittal shear waves if the absorptivity is large. As a result, the sensitivity of AA-based viscosity sensors to non-Newtonian properties of fluids must be substantially higher than of those using absorption of acoustic waves at an isolated solid–fluid interface [10–16]. This important feature of AA has also been investigated experimentally in paper [28] for the normally incident shear acoustic waves. This is the main reason why AA is of a special importance for the experimental investigation of non-Newtonian properties of fluids [28].

The main physical reason for the strong sensitivity of AA to non-zero relaxation time(s) in the fluid is related to the fact that due to strong absorption in the layer, the range of variations of the absorptivity

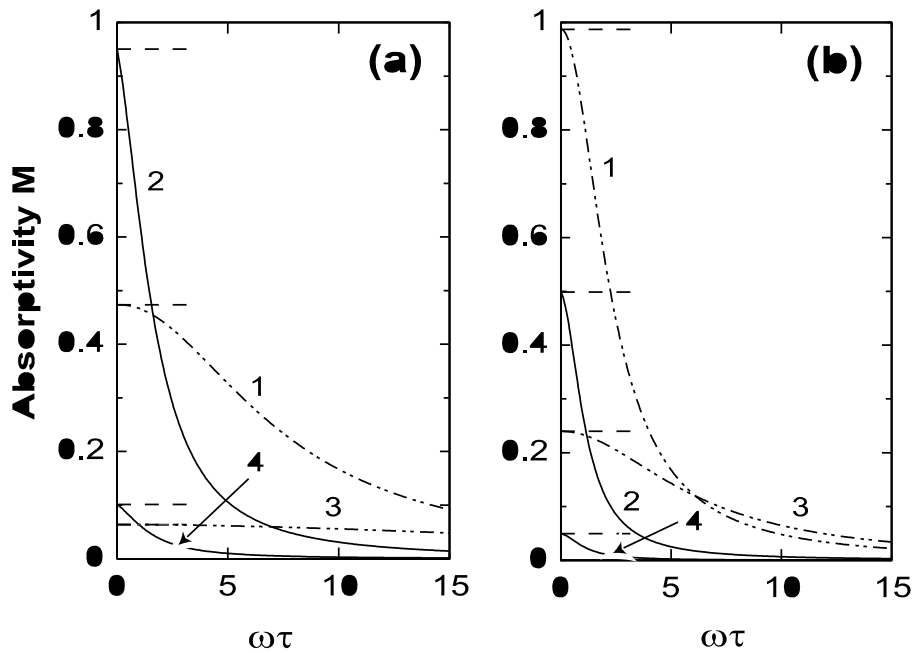


Figure 8: The dependencies of the absorptivity M on the product $\omega\tau$ for two different thicknesses of the layer: (a) $h = 1 \mu\text{m}$, (b) $h = 5 \mu\text{m}$. Curves 1: tin–poly-1-butene-16–silica, $\theta = \theta_{c1}(\text{tin}) \approx 38.504^\circ$. Curves 2: tin–poly-1-butene-16–silica, $\theta = 70^\circ$. Curves 3: silica–poly-1-butene-16–tin, $\theta = \theta_{c1}(\text{silica}) \approx 39.046^\circ$. Curves 4: silica–poly-1-butene-16–tin, $\theta = 70^\circ$. The dashed straight lines indicate the absorptivities for the corresponding Newtonian fluid layers (with the same as for poly-1-butene-16 viscosity and density, but with $\omega\tau \ll 1$)

is much larger (see curves 1 and 2 in Fig. 8a and b) than for an isolated solid–fluid interface [10,11]. Therefore, as was mentioned above during the discussion of Fig. 2, it is beneficial to use the structures with the second elastic medium being more rigid than the first, since in this case the absorptivity can be especially large—see Figs. 2 and 8a,b.

4 Conclusions

This paper has analysed the main features of the anomalous absorption of bulk shear sagittal waves in layers of Newtonian and non-Newtonian fluids between two different elastic media in the frictional contact approximation. The absorptivity in an ultra-thin fluid layer of thickness, that is much smaller than the wavelength and penetration depths of longitudinal and shear acoustic waves in the fluid, has been demonstrated to be much larger than the absorptivity of bulk acoustic waves at an isolated solidfluid interface. An interesting behaviour that is characterized by pronounced maximums in the angular dependencies of the absorptivity has been demonstrated and investigated numerically for various structural parameters including layer thickness. In particular, it has been shown that strong and sharp absorptivity maximums occur at two critical angles of incidence at which the reflected and transmitted longitudinal waves in the surrounding elastic media propagate parallel to the layer. An important and unique feature of AA of sagittal shear waves is that these two strong maximums of the absorptivity coincide with simultaneous strong maximums of the optimal layer thickness. This fact may be important for the experimental observation and applications of AA for the analysis of fluid layers with small viscosity, where the optimal layer thicknesses may be unreasonably small. The effect of small variations in parameters of the elastic media on the absorptivity maximums has been analysed.

It has been demonstrated theoretically that one of the most important features of AA is its much higher sensitivity to non-Newtonian properties of fluids (i.e., non-zero times(s) of relaxation of shear stresses in viscous fluids) than that of the absorption of acoustic waves at an isolated solid–fluid in-

terface. The stronger the anomalous absorption, the stronger its sensitivity to non-Newtonian properties of the fluid layer. This makes AA especially important for the experimental investigation of non-Newtonian properties of fluids and particularly solid–fluid interfaces.

The developed frictional contact approximation has been shown to be very useful for simple analysis of AA in non-uniform fluid layers with fluid parameters (i.e., density, viscosity, and/or relaxation times) varying across the layer. This is important for the analysis of interactions (e.g., adsorption–desorption processes) at solid–fluid interfaces, resulting in stratification of the fluid in the vicinity of a solid surface.

As a result, feasible applications of AA of acoustic waves can be anticipated in such areas as investigation and diagnostics of ultra-small amounts of fluids (less than $\approx 10^{-5}\text{cm}^3$), suspensions, colloidal solutions, biological and human fluids, solidfluid interfaces, frictional contacts and lubricants in tribology, non-destructive evaluation, etc.

Acknowledgements

The authors gratefully acknowledge financial support for this work from the Queensland University of Technology.

References

1. J.-M. Baik, R.B. Thompson, Ultrasonic scattering from imperfect interfaces: a quasi-static model, *J. Nondestruct. Eval.* 4 (1984) 177–196.
2. F.J. Margetan, R.B. Thompson, T.A. Gray, Interfacial spring model for ultrasonic interactions with imperfect interfaces: theory of oblique incidence and application to diffusion-bonded butt joints, *J. Nondestruct. Eval.* 7 (1988) 131–152.
3. P.B. Nagy, L. Adler, Ultrasonic NDE of solid-state bonds: internal and friction welds, *J. Nondestruct. Eval.* 7 (1988) 199–215.
4. P.B. Nagy, Ultrasonic classification of imperfect surfaces, *J. Nondestruct. Eval.* 11 (1992) 127–139.
5. A.I. Lavrentyev, S.I. Rokhlin, Ultrasonic spectroscopy of imperfect contact interfaces between a layer and two solids, *J. Acoust. Soc. Am.* 103 (1998) 657–664.
6. A.L. Shuvalov, J. Lothe, The Stroh formalism and the reciprocity properties of reflection-transmission problems in crystal piezo-acoustics, *Wave Motion* 25 (1997) 331–345.
7. A.L. Shuvalov, A.S. Gorkunova, Cutting-off effect at reflection-transmission of acoustic waves in anisotropic media with sliding-contact interfaces, *Wave Motion* 30 (1999) 345–365.
8. S.I. Rokhlin, Y.J. Wang, Analysis of boundary conditions for elastic wave interaction with an interface between two solids, *J. Acoust. Soc. Am.* 89 (1991) 503–515.
9. S.I. Rokhlin, Y.J. Wang, Equivalent boundary conditions for thin orthotropic layer between two solids: reflection, refraction, and interface waves, *J. Acoust. Soc. Am.* 91 (1992) 1875–1887.
10. A.J. Barlow, R.A. Dickie, J. Lamb, Viscoelastic relaxation in poly-1butenes of low molecular weight, *Proc. Roy. Soc. A* 300 (1967) 356–372.
11. R.S. Moore, H.G. McSkimin, in: *Physical Acoustics*, vol. 6, Academic Press, New York, 1970, pp. 167–243.
12. A.J. Ricco, S.J. Martin, Acoustic wave viscosity sensor, *Appl. Phys. Lett.* 50 (1987) 1474–1476.

13. T.M. Niemczyk, S.J. Martin, G.C. Frye, A.J. Ricco, Acousto-electric interaction of plate modes with solutions, *J. Appl. Phys.* 64 (1988) 5002–5008.
14. T. Sato, H. Okajima, Y. Kashiwase, R. Motegi, H. Nakajima, Shear horizontal acoustic plate mode viscosity sensor, *Jpn. J. Appl. Phys.* 32 (5B1) (1993) 2392–2395.
15. V. Shah, K. Balasubramaniam, Effect of viscosity on ultrasound wave reflection from a solid/liquid interface, *Ultrasonics* 34 (1996) 817–824.
16. M. Thompson, G.K. Dhaliwal, C.L. Arthur, G.S. Calabreses, The potential of the bulk acoustic wave device as a liquid-phase immunosensor, *IEEE Trans. UFFC-34* (2) (1987) 127–135.
17. M. Schoenberg, Elastic wave behaviour across linear slip interfaces, *J. Acoust. Soc. Am.* 68 (1980) 1516–1521.
18. O. Lenoir, J.-L. Izbicki, M. Rousseau, F. Coulouvrat, Subwavelength ultrasonic measurement of a very thin fluid layer thickness in a trilayer, *Ultrasonics* 35 (1997) 509.
19. L.M. Brekhovskikh, *Waves in Layered Media*, Academic, London, 1960.
20. A.G. Every, G.L. Koos, J.P. Wolfe, Ballistic phonon imaging in sapphire: bulk focusing and critical-cone channelling effects, *Phys. Rev. B* 29 (1984) 2190–2209.
21. D.K. Gramotnev, S.N. Ermoshin, L.A. Chernozatonskii, Anomalous absorption of shear waves in transmission across a gap filled with viscous fluid, *Akust. Zh.* 37 (1991) 660–669, *Sov. Phys. Acoust.* 37 (1991) 343–348.
22. M.L. Vyukov, D.K. Gramotnev, L.A. Chernozatonskii, Anomalous absorption of shear acoustic waves in a multi-layer structure with fluid, *Akust. Zh.* 37 (1991) 448–454, *Sov. Phys. Acoust.* 37 (1991) 229–233.
23. L.A. Chernozatonskii, D.K. Gramotnev, M.L. Vyukov, Anomalous absorption of sagittal shear waves by a thin fluid layer, *J. Physics D* 25 (1992) 226–233.
24. L.A. Chernozatonskii, D.K. Gramotnev, M.L. Vyukov, Anomalous absorption of longitudinal acoustic waves by a thin layer of viscous fluid, *Phys. Lett. A* 164 (1992) 126–132.
25. D.K. Gramotnev, M.L. Vyukov, Anomalous absorption of shear plate modes by a thin layer of viscous fluid, *Int. J. Mod. Phys. B* 8 (1994) 1741–1764.
26. D.K. Gramotnev, M.L. Mather, Anomalous absorption of shear acoustic waves by a thin layer of non-Newtonian fluid, *J. Acoust. Soc. Am.* 106 (1999) 2552–2559.
27. D.K. Gramotnev, M.L. Mather, T.A. Nieminen, Anomalous absorption of bulk longitudinal acoustic waves in a layered structure with viscous fluid, in: *Proceedings of the 1998 IEEE Ultrasonics Symposium, 1998*, pp. 1203–1206.
28. M.J. Lwin, D.K. Gramotnev, M.L. Mather, J.M. Bell, W. Scott, Experimental observation of anomalous absorption of bulk shear acoustic waves by a thin layer of viscous fluid, *Appl. Phys. Lett.* 76 (2000) 2020–2022.